Tellus (1983), *35A*, 119–135

Theoretical study of multiple equilibria in simple axisymmetric tropical circulations

By B. N. GOSWAMI, *National Research Council, Washington, DC, and Laboratory for Atmospheric Sciences, NASA/Goddard Space Flight Center, Greenbelt, MD 20771, U.S.A.*

(Manuscript received January 19; in final form May 3, 1982)

ABSTRACT

Possible existence of multiple equilibria in axisymmetric circulation is examined using simple models. A simple two-layer axisymmetric model is constructed using balance equations on an equatorial beta-plane. The model has no mountains and the thermal forcing is represented by a Newtonian cooling law. A radiative equilibrium temperature distribution is prescribed that has a maximum around 25° latitude, intended to simulate the summer conditions in the northern hemisphere. The effect of heating due to condensation is included only through the change in the static stability parameter. A host of steady state solutions are obtained analytically from a severely truncated version of this model. An analysis of stability of these steady states with respect to first and second y-mode perturbations reveal that only one steady state is stable against both types of perturbation. Two other steady states are found to be quasi-stable (e-folding time greater than three weeks) with respect to these perturbations.

We then examined two different simple numerical models for possible existence of multiple equilibria in symmetric circulations. First, the time dependent spectral equations for the above two-layer model, with many more degrees of freedom, were numerically integrated with various initial conditions given by the steady state solutions for the severely truncated model. These integrations show that the model gives only one steady state corresponding to the stable state given by the truncated model. Secondly, a multi-level grid point model developed by Kalnay-Rivas (1973) was examined. This model uses primitive equations under Boussinesq approximations. Parameterizations for thermal forcing and dissipation used in this model were similar to those used in the spectral model. It is found by integrating this model for various initial conditions that this model also gives only one steady state similar to the steady state obtained by the spectral model. The inability of these simple models to exhibit multiple equilibria in axisymmetric circulations is discussed.

1. Introduction

In recent studies by Charney and DeVore (1979) and Charney and Straus (1980) evidence has been presented that the large-scale atmospheric motion is capable of possessing a multiplicity of equilibrium states of which more than one may be stable. Charney and DeVore (1979) studied the flow of a forced barotropic fluid over a wavy topography in a beta-plane channel. For a certain range of forcing, they showed that there exist two stable and one unstable equilibrium states. One of the stable equilibrium states has strong zonal flow and weak wave perturbation, while the other stable state has weak zonal flow and strong wave perturbation. The unstable state has intermediate zonal flow. The state with weak zonal flow and strong wave perturbation resembles, in certain ways, a mid-latitude blocking situation. They also confirmed the existence of the two stable equilibrium states by numerical integration of a grid-point model with many more degrees of freedom than the spectral model. Charney and Straus (1980) extended this study to include baroclinic effects by considering a two-layer model. Both of these studies use quasi-geostrophic equations and hence the results are not strictly applicable to the tropical circulation. In the present paper we propose to examine the question of

 0280-6495/83/020119-17$02.50/0

whether the axisymmetric part of the atmospheric circulation can possess more than one equilibrium state. The motivation for this study is twofold. First, from a purely theoretical point of view, it is important to know if, for a given forcing and dissipation, an axisymmetric flow can possess more than one equilibrium solution. Second, from a practical point of view, we believe that such a study has some relevance in understanding certain features of the tropical circulation. We shall elaborate this point a little later.

Symmetric models have been studied extensively during recent years (Charney, 1969; Hunt, 1973; Schneider and Lindzen, 1977; Schneider, 1977; Held and Hou, 1980). These studies were not aimed at simulating the earth's general circulation in detail but were used to understand certain features of the general circulation without having to deal with the complex zonally asymmetric transients. In particular, an axisymmetric model is expected to contain most of the dynamics of the tropical circulation since the transports of heat and momentum in the low-latitude atmosphere are dominated by the mean meridional circulation rather than by the transient eddies (Oort and Rasmusson, 1971). It is interesting to note that in one study (Charney, 1969) in which a symmetric model was used to study the dynamics of the ITCZ, the author noted that for the same thermal driving and physical parameters he could obtain different steady states by simply varying the initial conditions. In particular, it was noticed that, by changing the initial conditions, the position of the ITCZ could be obtained in almost any location within a certain range of latitudes. To our knowledge, this is the first reference to the possible existence of multiple equilibrium states in a symmetric model.

As we mentioned earlier, the multiplicity of the equilibrium states of a symmetric model may have some relevance in understanding some features of the tropical circulation. There exists some observational evidence (Sikka and Gadgil, 1980) to indicate that the active and break phases of the South Asian summer monsoon may be two different equilibrium states of the tropical atmosphere. The large-scale circulation during these two phases are distinctly different (Ramamurthy, 1969) and the transition time from one to the other is short compared to their durations. The active phases of the monsoon are characterized by a convergence zone and rainfall over central India associated with what is known as the monsoon trough. The rainfall during this phase is normally enhanced by a series of depressions that form over the Bay of Bengal and move north-northwest. During the break phases, the monsoon trough either disappears or moves northward to the foothills of the Himalayas. Moreover, the depressions do not form during the break periods. However, southern India gets a considerable amount of rain during the break periods and sometimes even a trough is seen between the equator and 15° N. In spectral study of various observed fields, the active and break epochs show up as a low frequency quasi-biweekly mode (Keshavamurty, 1973; Murakami, 1976; Krishnamurti and Bhalme, 1976). These features are very clearly revealed in recent satellite cloud picture studies (Sikka and Gadgil, 1980; Yashunari, 1979). It is seen from these studies that there are two distinct cloud bands, one associated with the oceanic convergence zone and the other associated with a continental convergence zone (monsoon trough). The onset and regeneration of the continental cloud band is triggered by northward movement of the oceanic cloud band. However, they are complementary in character. In other words, when the continental convergence zone is active, the oceanic one is absent or weak (an active phase) and vice versa. If the active and break phases of the monsoon are to be considered as two different equilibrium states, the transition from one to the other has to be triggered by a large amplitude perturbation on the basic state. This, we believe, is accomplished by the monsoon depressions and the associated cloud-radiation feedback. A qualitative explanation of transition from active to break phase was given by Krishnamurti and Bhalme (1976). According to them, during the initial stage, strong solar insolation and lack of cloud cover gives rise to shallow convection. This restores conditional instability and enhances the monsoon trough. This situation favors formation of monsoon depressions. These depressions give rise to increase in cloud cover. The enhanced cloud cover reduces insolation and stabilizes the lower atmosphere. Thus, the stage is set for a break phase to set in. During the break the cloud cover disappears and insolation again starts acting to restore the active phase.

Numerical general circulation models have been used in a large number of studies (Washington and Daggupaty, 1975; Krishnamurti et al., 1973; Hahn and Manabe, 1975; Gilchrist, 1977) to investigate the monsoon circulation. These studies have met with various degrees of success in simulating the monsoon circulation. In contrast to these complex general circulation models, some simple models have also been able to simulate the essential features of the monsoon circulation with great success (Webster et al., 1977; Webster and Chou, 1980a, b). Hahn and Manabe (1975) emphasize that the Himalayan mountains play an important role in maintaining the monsoon circulation. On the other hand, Webster and Chou (1980a, b) included a simple interactive ocean in their simple axisymmetric, two-layer model but they did not have the topography. Even with this simple model they were able to reproduce some of the basic features of the monsoon including the quasi-biweekly periodicity. While it is clear from all these studies that the mountains, the land-ocean contrasts, the hydrology cycle and the thermal heating all play important roles in driving the monsoon circulation, it is not clear which one of them has a dominating effect over the others.

The aim of the present study is not to clarify which is the dominating driving mechanism for the tropical circulation but to examine whether an axisymmetric model with simple driving could sustain more than one equilibrium solution. The model used for this study is a two-layer, axisymmetric, balanced model in a beta-plane geometry centered around the equator. A modified balanced set of equations is used in which the zonal velocity is assumed to be in geostrophic balance while the meridional velocity is prognostically determined. Such a balance set was also used by Bates (1970) to calculate the basic state for his ITCZ study. The basic driving for the symmetric motion are the radiative and convective heat sources and sinks. The radiative heating is modeled as a Newtonian cooling linear law. A radiative equilibrium temperature distribution is prescribed. The release of latent heat due to condensation is also parameterized in a very simple way. We assume that the tropical atmosphere is always in a saturated state and any ascending motion results in condensation. The energy released this way is assumed to be uniformly distributed throughout the column of air. It is also assumed that, associated with any descending motion, there is an equivalent amount of cooling. We realize that this assumption is unrealistic. However, this representation was necessary so that we could express the heating in terms of a finite number of orthogonal functions for analytic calculations. The model equations are solved by representing the variables in terms of a set of orthogonal functions. The orthogonal functions used in this study are the parabolic cylinder functions. It is found that for this model, there exists only one *stable* equilibrium state. The model, however, shows that there exist a number of unstable equilibrium states.

We also examined the possibility of existence of multiple equilibria in a multi-level zonally symmetric model. For this purpose we chose a model developed by Kalnay-Rivas (1973). This is a primitive equation grid point model under Boussinesq approximation. With parameterizations for thermal forcing and dissipation similar to ones used in the spectral model, this model was also integrated for various initial conditions. However, this model also gives only one steady state. This steady state is similar to the one obtained from the two-layer spectral model.

The simple axisymmetric models used in this study with simple forcings and dissipation fail to show the existence of multiple equilibria in symmetric circulations. Whether the active and break monsoons can be considered as two equilibrium states of the tropical atmosphere, therefore, remains to be answered.

2. The model

The model is a two-layer axisymmetric balanced model. A beta-plane geometry centered around the equator is used. Writing the momentum equation and the continuity equation at the upper and lower levels, the thermodynamic equation and the hydrostatic relation at the center of the two levels and using central differencing in the vertical, the basic equations for the two-layer model can be expressed as,

$$\frac{\partial u_1}{\partial t} + v_1 \frac{\partial u_1}{\partial y} + \frac{\omega_2}{2\Delta p}(u_3 - u_1) - \beta y v_1 = (F_x)_1, \tag{2.1}$$

$$\frac{\partial u_3}{\partial t} + v_3 \frac{\partial u_3}{\partial y} + \frac{\omega_2}{2\Delta p}(u_3 - u_1) - \beta y v_3 = (F_x)_3, \tag{2.2}$$

$$\beta y u_1 = -\frac{\partial \phi_1}{\partial y}, \tag{2.3}$$

$$\beta y u_3 = -\frac{\partial \phi_3}{\partial y}, \tag{2.4}$$

$$\frac{\partial v_1}{\partial y} + \frac{\omega_2}{\Delta p} = 0, \tag{2.5}$$

$$\frac{\partial v_3}{\partial y} - \frac{\omega_2}{\Delta p} = 0, \tag{2.6}$$

$$\phi_1 - \phi_3 = RT_2, \tag{2.7}$$

$$\frac{\partial}{\partial t}(\phi_1 - \phi_3) - S\omega_2 = \frac{R}{C_p} Q_2, \tag{2.8}$$

where

$$S = \left(\frac{1}{p_2}\,\frac{\theta_1 - \theta_3}{\theta_2}\right)_s$$

is the stability parameter, $(F_x)_{1,3}$ are the frictional forces at the upper and the lower layers and Q_2 is the diabatic heating rate. The other symbols have their usual meaning (see Bates, 1970). The subscripts 1, 2, and 3 refer to the 250 mb, 500 mb, and 750 mb surfaces, respectively. In writing eqs. (2.1)–(2.8), we have assumed that the vertical velocity is zero at the top and the bottom of the atmosphere. We have also assumed a no stress top boundary condition. At the bottom boundary, the stress will be expressed by a drag law. If we assume that v_1 and v_3 vanish at the lateral boundaries of the channel, it is easy to show from eqs. (2.5) and (2.6) that $v_1 = -v_3$. We impose a constraint on v, namely that there is no cross-equatorial flow. In other words $v = 0$ at $y = 0$. This demands that v be an anti-symmetric function about the equator. If v is anti-symmetric about the equator, eqs. (2.1)–(2.8) also demand that u, T, ω, and ϕ be symmetric about the equator.

It can be shown that in the absence of dissipation and generation the system of eqs. (2.1)–(2.8) conserve the total energy of the system. If we define the total energy E as

$$E = (u_1^2 + u_3^2)/2 + (\phi_1 - \phi_3)^2/C,$$

where $C = Sp_2$, it is easy to show by using the boundary condition that $v = 0$ at $y = \pm W$, that,

$$\frac{d}{dt}\int_{-W}^{W} E\,dy = 0.$$

2.1. *Frictional forces*

The frictional force is given by,

$$\mathbf{F} = -g\frac{\partial \boldsymbol{\tau}}{\partial p},$$

where the stress $\boldsymbol{\tau}$ can be written as

$$\boldsymbol{\tau} = \begin{cases} \mu \dfrac{\partial \mathbf{V}}{\partial Z}, & \text{in the interior} \\ C_D \rho_4 |\mathbf{V}_3| \mathbf{V}_3, & \text{near the ground} \end{cases}$$

μ being the coefficient for vertical eddy viscosity and C_D the drag coefficient. Thus,

$$(F_x)_1 = -k_i(u_1 - u_3) \tag{2.9}$$

and

$$(F_x)_3 = k_i(u_1 - u_3) - Au_3, \tag{2.10}$$

where

$$k_i = (g\mu)/(p_2\,\Delta Z_{13}), \quad A = C_D\, g\rho_4 |\bar{u}_3| / p_2,$$

where $|\bar{u}_3|$ is the standard value of zonal wind near the ground.

The value of the internal friction parameter used in this study is the same as the one used by Bates (1970), i.e. $k_i = 0.48 \times 10^{-6}$ s^{-1}. The coefficient of vertical eddy viscosity used in calculating k_i is $\mu = 200$ g cm^{-1} s^{-1}. Similarly, the value of surface friction parameter used in this study is $A = 2.044 \times 10^{-6}$ s^{-1}. This value of A is arrived at by using $C_D = 0.002$ and a value of $|\bar{u}_3| = 7$ m s^{-1}. This means that the frictional relaxation time constant due to internal friction is about 24 days while that due to the surface friction is about 6 days.

2.2. *Heating terms*

The diabatic heating rate Q_2 contains a contribution from radiative heating as well as convective heating. Assuming that the atmosphere is transparent to solar radiation and tends to a state of radiative equilibrium with the underlying surface (assumed to be all ocean), the radiative cooling can be written as a Newtonian law of the form

$$(Q_2)_r = k_r C_p (T_e - T_2), \tag{2.11}$$

where $1/k_r$ is a radiative relaxation time constant (Bates, 1970) given by

$$k_r = (4R\sigma T_4^4)/(C_p \rho_4 g \Delta Z_{13}). \tag{2.12}$$

A value of $k_r = 0.8468 \times 10^{-6}$ s^{-1} or $k_r = (14$ days$)^{-1}$ is used in this study. The radiative equilibrium temperature T_e will be specified.

In order to calculate the convective heating rate, we note that $v_1 = -v_3$ in our model. In other words, the convergence at the lower level is equal to the divergence at the upper level or vice versa. Assuming that the mixing ratio decreases exponentially with height, there will be a net convergence (or divergence) of moisture in a given column of air. Also assuming that the air is always near saturation this moisture is assumed to be rained out immediately. The latent heat released is then assumed to be distributed uniformly in the vertical column. This process can be parameterized as

$$\frac{R}{C_p}(Q_2)_c = -S\eta F(\omega_2)\,\omega_2, \tag{2.13}$$

where

$$\eta = \left(\frac{Lq_4}{\gamma C_p T_{2s}}\right) \bigg/ \left(\frac{\theta_1 - \theta_3}{\theta_2}\right)_s \tag{2.14}$$

and

$$F(\omega_2) = \{1 + \exp(\hat{D}\omega_2)\}^{-1} \tag{2.15}$$

In eq. (2.14), γ is a constant such that the relative humidity distribution can be represented by

$$q(p) = q_4 \exp\left\{-\gamma\left(1 - \frac{p}{p_4}\right)\right\}$$

where q_4 is the relative humidity near the ground. In eq. (2.15), $\hat{D}$ is a large number. $F(\omega_2)$ is essentially a smoothing function such that for $\omega_2 < 0$ (ascending motion) $F(\omega_2) \approx 1$ and for $\omega_2 > 0$ (descending motion) $F(\omega_2) \approx 0$. However, this expression is not suitable for representation in terms of a finite number of orthogonal functions. Thus, in our spectral representation we shall put $\hat{D} = 0$ implying that ascending motion is associated with heating while descending motion is associated with cooling. We realize that this is a simple minded representation of convective processes. Nevertheless, this representation will be tried as a first approximation. Thus, eq. (2.8) can be written as

$$\frac{\partial}{\partial t}(\phi_1 - \phi_3) - S(1 - \eta)\,\omega_2 = k_r R(T_e - T_2) \tag{2.16}$$

It is clear from eq. (2.16) that the parameterization for convective heating used in this study only reduces the magnitude of the static stability parameter. Physically this effect can be understood as follows: a parcel of ascending air is associated with adiabatic cooling represented by the term $-S\omega_2$. However, the condensation of moisture carried by the ascending parcel releases an amount of latent heat represented by the term $S\eta\omega_2$. The result is that the total amount of cooling in a column of air is reduced by the condensational heating. Therefore, the system of eqs. (2.1)–(2.7) and eq. (2.16) can be reduced to three independent equations given by

$$\frac{\partial}{\partial t}\left(y\frac{\partial \phi_1}{\partial y}\right) - v_3\left(y\frac{\partial^2 \phi_1}{\partial y^2} - \frac{\partial \phi_1}{\partial y}\right) - \frac{1}{2}y\frac{\partial v_3}{\partial y}\frac{\partial}{\partial y}(\phi_1 - \phi_3) - \beta^2 y^3 v_3 = k_i y\frac{\partial}{\partial y}(\phi_3 - \phi_1), \tag{2.17}$$

$$\frac{\partial}{\partial t}\left(y\frac{\partial \phi_3}{\partial y}\right) + v_3\left(y\frac{\partial^2 \phi_3}{\partial y^2} - \frac{\partial \phi_3}{\partial y}\right) - \frac{1}{2}y\frac{\partial v_3}{\partial y}\frac{\partial}{\partial y}(\phi_1 - \phi_3) + \beta^2 y^3 v_3 = -k_i y\frac{\partial}{\partial y}(\phi_3 - \phi_1) - Ay\frac{\partial \phi_3}{\partial y}, \tag{2.18}$$

$$Dy\frac{\partial^2 v_3}{\partial y^2} + v_3\left[-y\frac{\partial^2}{\partial y^2}(\phi_1 + \phi_3) + \frac{\partial}{\partial y}(\phi_1 + \phi_3) - 2\beta^2 y^3\right] = Ay\frac{\partial \phi_3}{\partial y} + (k_r - 2k_i)\,y\frac{\partial}{\partial y}(\phi_1 - \phi_3) - yk_r R\frac{\partial T_e}{\partial y}. \tag{2.19}$$

where $D = C(1-\eta)$. The diagnostic equation (2.19) is obtained by using eqs. (2.17) and (2.18) to eliminate the time-dependent terms in eq. (2.16).

It would be convenient for subsequent calculations to normalize the variables in eqs. (2.17)–(2.19). For this purpose, we introduce a basic length scale $L = a/2$ and a basic time scale $T = 1/2\Omega$. Thus, $y = 2y'/a$; $(u, v) = (u', v')/a\Omega$; $\phi = \phi/a^2\Omega^2$; $t = 2\Omega t'$, $k_i = k_i'/2\Omega$, $k_r = k_r'/2\Omega$, $A = A'/2\Omega$, $C = C'/a^2\Omega^2$, $R = R'/a^2\Omega^2$, $\beta = a\beta'/4\Omega$, where the prime refers to the dimensional quantities. In terms of these non-dimensional quantities, the eqs. (2.17)–(2.19) remain the same in form. However, we now have to give the initial conditions and the physical parameters in non-dimensional form.

3. Linear solutions

In this section we shall solve for the linear steady states for various prescribed forcings. The linear equations are

$$\frac{\partial u_1}{\partial t} + \beta y v_3 = -k_i(u_1 - u_3), \tag{3.1}$$

$$\frac{\partial u_3}{\partial t} - \beta y v_3 = k_i(u_1 - u_3) - Au_3, \tag{3.2}$$

$$\frac{\partial}{\partial t}(\phi_1 - \phi_3) - D\frac{\partial v_3}{\partial y} = k_r[RT_e - (\phi_1 - \phi_3)]. \tag{3.3}$$

Using the geostrophic relations (eqs. (2.3) and (2.4)) and eliminating ϕ_1, and ϕ_3 from eq. (3.3) we get a diagnostic equation given by

$$D\frac{\partial^2 v_3}{\partial y^2} - 2\beta^2 y^2 v_3 = -k_r R\frac{\partial T_e}{\partial y} - 2\beta y(2k_i - k_r)(u_1 - u_3) - \beta y A u_3. \tag{3.4}$$

Let us now introduce a set of new variables defined by

$$U = (u_1 + u_3)/2$$

$$W = (u_1 - u_3)/2$$

and

$$V = v_3$$

Thus, eqs. (3.1), (3.2) and (3.4) can be written as

$$\frac{\partial U}{\partial t} = -\frac{A}{2}(U - W), \tag{3.5}$$

$$\frac{\partial W}{\partial t} + \beta y V = -2k_i W + \frac{A}{2}(U - W) \tag{3.6}$$

and

$$D\frac{\partial^2 V}{\partial y^2} - 2\beta^2 y^2 V = -k_r R\frac{\partial T_e}{\partial y} - 2\beta y(2k_i - k_r)W - \frac{A}{2}\beta y(U - W). \tag{3.7}$$

In steady state, eq. (3.5) gives $U - W = 0$ or $u_3 = 0$ and eq. (3.7) reduces to

$$\frac{\mathrm{d}^2 V}{\mathrm{d}y^2} - K_1 y^2 V = K_2 y W^* \tag{3.8}$$

where $k_1 = \beta^2 k_r/Dk_i$, $K_2 = 2\beta k_r/D$ and

$$W^*(y) = -\frac{R}{2\beta y}\frac{\partial T_e(y)}{\partial y} \tag{3.9}$$

Introducing a transformation of the type $\zeta = k_1^{1/4} y$, eq. (3.8) can be written as

$$\frac{\mathrm{d}^2 V}{\mathrm{d}\zeta^2} - \zeta^2 V = (K_2 K_1^{-3/4})\zeta W^*(y) \tag{3.10}$$

The solutions of the eigenvalue problem corresponding to eq. (3.10) are the parabolic cylinder functions (Abramovitch and Stegun, 1965; Cane and Sarachik, 1976), namely

$$F_n(\zeta) = \alpha_n H_n(\zeta)\exp(-\zeta^2/2)$$

with

$$\alpha_n = \pi^{1/4}(2^n n!)^{-1/2}, \tag{3.11}$$

where $H_n(\zeta)$ are Hermit polynomials. Keeping in mind that v is anti-symmetric about the equator, the general solution for the inhomogenous eq. (3.10) can be written as

$$V = \sum_{n\,\mathrm{odd}} V_n F_n(\zeta) \tag{3.12}$$

Let us now prescribe the radiative equilibrium temperature. The radiative equilibrium tempera-

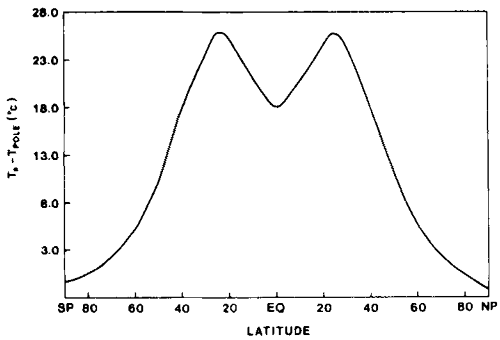

Fig. 1. The radiative equilibrium temperature distribution used for this study. This temperature distribution can be represented by $T_e(y) = (\alpha_0 T_0 + \alpha_2 T_2 H_2(y)) \exp(-y^2/2)$ where $T_0 = 40$, $T_2 = 20$, with α_0 and α_2 as defined in eq. (3.11).

ture is expressed in terms of two parabolic cylinder functions, namely

$$T_e(y) = [\alpha_0 T_0 + \alpha_2 T_2 H_2(y)] \exp(-y^2/2). \quad (3.13)$$

When we substitute eq. (3.13) into eq. (3.10) and express the right-hand side of eq. (3.10) in terms of the variable ζ, we get terms containing $H_{1,3}(\zeta) \exp(-K_1^{-1/2} \zeta^2/2)$. These terms are also expanded in terms of $F_n(\zeta)$. Then eq. (3.10) can be solved for various V_n by equating coefficients of $F_n(\zeta)$. Finally, V is obtained from eq. (3.12) by truncating the series appropriately. Fig. 2 shows the V and corresponding ul obtained by truncating the series after ten functions, i.e., $N = 19$. The non-dimensional parameters used in calculating this linear steady state are $A = 0.014$, $k_i = 0.0033$, $k_r = 0.0057$, $R = 0.0014$, $D = 0.0437$, $\eta = 0$, $\beta = 0.5$, $T_0 = 40$, and $T_2 = 20$. In dimensional form these parameters correspond to $A = 2.044 \times 10^{-6}$ s^{-1}, $k_i = 0.48 \times 10^{-6}$ s^{-1}, $k_r = 0.8468 \times 10^{-6}$ s^{-1}, $R = 287$ m^2 s^{-2} deg^{-1}, $D = 9.4545 \times 10^3$ m^2 s^{-2}. The radiative equilibrium temperature distribution for this calculation as well as for the non-linear calculations to be presented later is shown in Fig. 1. It is found that, adding more functions to represent V does not change the results significantly. In Section 6, this analytic solution is compared with numerical (linear) solution.

4. Spectral equations

We now express our variables ϕ_1, ϕ_3, v_3 as well as the radiative equilibrium temperature T_e in terms

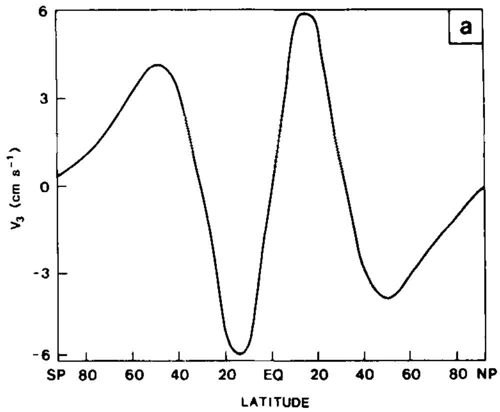

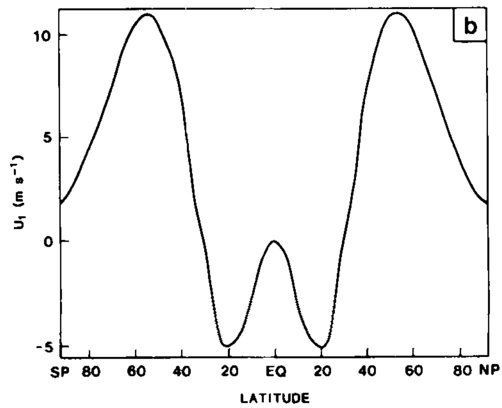

Fig. 2. (a) The meridional velocity at the lower layer (V_3) from the linear model. (b) Zonal wind distribution at the upper layer for the linear steady state. The physical parameters used to calculate this linear state are (in non-dimensional form) $A = 0.014$, $k_i = 0.0033$, $k_r = 0.0057$ and $D = 0.0437$.

of a set of orthogonal functions. We set

$$(\phi_1, \phi_3, T_e) = \sum_{j=0}^{J} (\phi_j^{(1)}, \phi_j^{(3)}, T_j) F_j; \quad j = 0, 2, \ldots, J \quad (4.1)$$

and

$$V_3 = \sum_{i=1}^{J+1} V_i F_i; \quad i = 1, 3, \ldots, J+1, \quad (4.2)$$

where F_n are parabolic cylinder functions given by

$$F_n(y) = \alpha_n H_n(y) \exp(-y^2/2) \quad (4.3)$$

with

$$\alpha_n = \pi^{1/4} (2^n n!)^{-1/2} \quad (4.4)$$

The F_n's are orthogonal, such that

$$\int_{-\infty}^{\infty} F_n F_m \, dy = \delta_{mn}.$$

We recall that our model demands ϕ_1, ϕ_3 (hence u_1 and u_3) and T_e to be symmetric about the equator while v_3 should be anti-symmetric about the equator (see Section 2). This is why we have represented ϕ_1, ϕ_3 and T_e in terms of even functions while v_3 is represented in terms of odd functions.

Substituting eqs. (4.1) and (4.2) in eqs. (2.17)–(2.19) we can write

$$\sum_{j=0}^{J} a_{jk} \dot{\phi}_j^{(1)} = \sum_{i=1}^{J+1} \sum_{j=0}^{J} X_{ijk} V_i \phi_j^{(1)} - \tfrac{1}{2} \sum_{i=1}^{J+1} \sum_{j=0}^{J} d_{ijk} V_i \phi_j^{(3)} + \beta^2 \sum_{i=1}^{J+1} e_{ik} V_i + k_i \sum_{j=0}^{J} a_{jk} (\phi_j^{(3)} - \phi_j^{(1)}), \tag{4.5}$$

$$\sum_{j=0}^{J} a_{jk} \dot{\phi}_j^{(3)} = \sum_{i=1}^{J+1} \sum_{j=0}^{J} X_{ijk} V_i \phi_j^{(3)} + \tfrac{1}{2} \sum_{i=1}^{J+1} \sum_{j=0}^{J} d_{ijk} V_i \phi_j^{(1)} - \beta^2 \sum_{i=1}^{J+1} e_{ik} V_i - k_i \sum_{j=0}^{J} a_{jk} (\phi_j^{(3)} - \phi_j^{(1)}) - A \sum_{j=0}^{J} a_{jk} \phi_j^{(3)} \tag{4.6}$$

and

$$\sum_{i=1}^{J+1} \sum_{j=0}^{J} Y_{ijk} V_i (\phi_j^{(3)} + \phi_j^{(1)}) + D \sum_{i=1}^{J+1} p_{ik} V_i - 2\beta^2 \sum_{i=1}^{J+1} e_{ik} V_i - A \sum_{i=0}^{J} a_{jk} \phi_j^{(3)} - (k_r - 2k_i) \times \sum_{j=0}^{J} a_{jk} (\phi_j^{(1)} - \phi_j^{(3)}) + k_r R \sum_{j=0}^{J} a_{jk} T_j = 0, \tag{4.7}$$

where $X_{ijk} = C_{ijk} - b_{ijk} + \tfrac{1}{2} d_{ijk}$ and $Y_{ijk} = b_{ijk} - C_{ijk}$, $i = 1, 3, \ldots, J+1$ and $j = 0, 2, \ldots, J$. The interaction coefficients are given by

$$a_{jk} = \overline{y F_k \frac{\partial F_j}{\partial y}}, \quad C_{ijk} = \overline{y F_k F_i \frac{\partial^2 F_j}{\partial y^2}},$$

$$e_{ik} = \overline{y^3 F_k F_i}, \quad b_{ijk} = \overline{F_k F_i \frac{\partial F_j}{\partial y}},$$

$$p_{ik} = \overline{y F_k \frac{\partial^2 F_i}{\partial y^2}}, \quad d_{ijk} = \overline{y F_k \frac{\partial F_i}{\partial y} \frac{\partial F_j}{\partial y}}. \tag{4.8}$$

The system of eqs. (4.5)–(4.7) consists of $J + 2$ ordinary differential equations in time represented by eqs. (4.5) and (4.6) and $J/2 + 1$ diagnostic equations represented by eq. (4.7). In the next section we shall seek steady state solutions of the system for a severely truncated representation.

5. Severely truncated steady state solutions

Let us assume that the system has attained a steady state such that $\partial/\partial t = 0$. In such a case, eqs. (4.5)–(4.7) reduce to a system of $3(J/2 + 1)$ bilinear algebraic equations. Ideally, we would like to know all the possible solutions of this system for an arbitrary J as that would tell us how many equilibrium states the system can possess. However, from a practical point of view, it is too formidable to obtain all the solutions for $J > 2$. Therefore, we shall consider a severely truncated system in which each variable is represented by only two orthogonal functions, i.e. $j, k = 0, 2$ and $i = 1, 3$. Let us define

$$Z_{ik} = D p_{ik} - 2\beta^2 e_{ik},$$

$$C_1 = k_r - 2k_i - A,$$

and

$$C_2 = k_r - 2k_i,$$

In this representation, eqs. (4.5)–(4.7) reduce to six bilinear equations, namely

$$(X_{100} V_1 + X_{300} V_3) \phi_0^{(1)} + (X_{120} V_1 + X_{320} V_3) \phi_2^{(1)} - \tfrac{1}{2}(d_{100} V_1 + d_{300} V_3) \phi_0^{(3)} - \tfrac{1}{2}(d_{120} V_1 + d_{320} V_3) \phi_2^{(3)} + k_i a_{00} (\phi_0^{(3)} - \phi_0^{(1)}) + k_i a_{20} (\phi_2^{(3)} - \phi_2^{(1)}) = -\beta^2 (e_{10} V_1 + e_{30} V_3) \tag{5.1}$$

$$(X_{100} V_1 + X_{300} V_3) \phi_0^{(3)} + (X_{120} V_1 + X_{320} V_3) \phi_2^{(3)} - \tfrac{1}{2}(d_{100} V_1 + d_{300} V_3) \phi_0^{(1)} - \tfrac{1}{2}(d_{120} V_1 + d_{320} V_3) \phi_2^{(1)} + k_i a_{00} (\phi_0^{(3)} - \phi_0^{(1)}) + k_i a_{20} (\phi_2^{(3)} - \phi_2^{(1)}) + A (a_{00} \phi_0^{(3)} + a_{20} \phi_2^{(3)}) = -\beta^2 (e_{10} V_1 + e_{30} V_3) \tag{5.2}$$

$$D(p_{10} V_1 + p_{30} V_3) + k_r a_{00} (\phi_0^{(3)} - \phi_0^{(1)}) + k_r a_{20} (\phi_2^{(3)} - \phi_2^{(1)}) + k_r R a_{00} T_0 + k_r R a_{20} T_2 = 0, \tag{5.3}$$

$$(X_{102} V_1 + X_{302} V_3)\,\phi_0^{(1)} + (X_{122} V_1 + X_{322} V_3)\phi_2^{(1)}$$
$$- \tfrac{1}{2}(d_{102} V_1 + D_{302} V_3)\,\phi_0^{(3)}$$
$$- \tfrac{1}{2}(d_{122} V_1 + d_{322} V_3)\,\phi_2^{(3)} + k_i\,a_{02}(\phi_0^{(3)} - \phi_0^{(1)})$$
$$+ k_i\,a_{22}(\phi_2^{(3)} - \phi_2^{(1)}) = -\beta^2(e_{12} V_1 + e_{32} V_3) \quad (5.4)$$

$$(X_{102} V_1 + X_{302} V_3)\,\phi_2^{(3)} + (X_{122} V_1 + X_{322} V_3)\,\phi_2^{(3)}$$
$$- \tfrac{1}{2}(d_{102} V_1 + d_{302} V_3)\,\phi_0^{(1)}$$
$$- \tfrac{1}{2}(d_{122} V_1 + d_{322} V_3)\,\phi_2^{(1)} + k_i a_{02}(\phi_0^{(3)} - \phi_0^{(1)})$$
$$+ k_i\,a_{22}(\phi_2^{(3)} - \phi_2^{(1)}) + A(a_{02}\,\phi_0^{(3)} + a_{22}\,\phi_2^{(3)})$$
$$= -\beta^2(e_{12} V_1 + e_{32} V_3), \quad (5.5)$$

$$D(p_{12} V_1 + p_{32} V_3) + k_r\,a_{02}(\phi_0^{(3)} - \phi_0^{(1)})$$
$$+ k_r\,a_{22}(\phi_2^{(3)} - \phi_2^{(1)}) + k_r R a_{02}\,T_0$$
$$+ k_r\,R a_{22}\,T_2 = 0. \quad (5.6)$$

Eqs. (5.1) and (5.2) have been used in writing eq. (5.3). Similarly, eqs. (5.4) and (5.5) have been made use of in writing eq. (5.6). The common roots of this system of six coupled equations are the steady state solutions of the severely truncated system. The common roots of this system of equations are obtained by making use of the bilinear property of eqs. (5.1), (5.2), (5.4), and (5.5).

If we assume that v_1 and v_3 are given, eqs. (5.1), (5.2), (5.4) and (5.5) can be written as four linear equations in $\phi_0^{(1)}$, $\phi_2^{(1)}$, $\phi_0^{(3)}$ and $\phi_2^{(3)}$. The equations can then be solved by standard matrix methods. Once $\phi_0^{(1)}$, $\phi_2^{(1)}$, $\phi_0^{(3)}$ and $\phi_2^{(3)}$ are known, the left-hand sides of eqs. (5.3) and (5.6) can be evaluated for the given v_1 and v_3. If the left-hand sides of both the eqs. (5.3) and (5.6) are zeros, we have a common root. However, for arbitrary values of v_1 and v_3 they will not be zeros. Therefore, for a given v_1 we vary v_3 over a wide range of values and find the values of v_3 for which the left-hand side of eq. (5.3) changes sign. This procedure is repeated for a wide range of values of v_1. Then the values of v_3 for which the left-hand side of eq. (5.3) changes sign are plotted against v_1. A similar graph is plotted for eq. (5.6). In Fig. 3, we present such solutions of eq. (5.3) and (5.6). The solid curve represents solution of eq. (5.3), while the dotted curve represents solution of eq. (5.6). The physical parameters (in non-dimensional form) used in these solutions are $A = 0.14 \times 10^{-1}$, $k_i = 0.33 \times 10^{-2}$, $k_r = 0.57 \times 10^{-2}$, $R = 0.14 \times 10^{-2}$, $\beta = 0.5$ and $D = 0.0437$. v_1 and v_3 corresponding to the intersections (together with corresponding $\phi_0^{(1)}$, $\phi_2^{(1)}$, $\phi_0^{(3)}$ and $\phi_2^{(3)}$) of the solid curves and the dotted curves represent common roots of the system of eqs. (5.1)–(5.6). Having obtained the approximate locations of the common solutions in this manner, the exact solutions can be obtained by fine tuning v_1 and v_3 near the intersections. The common roots of eqs. (5.1)–(5.6) thus obtained, are presented in Table 1. Note that we have presented six steady states in Table 1, while only three intersections are seen in Fig. 3. The other three roots are found by examining wider regions for v_1 and v_3.

Charney and Straus (1980) proposed a somewhat different scheme for solving a similar set of equations. As a test of accuracy of the method presented above, we also solved the set of eqs. (5.1)–(5.6) by using the scheme proposed by Charney and Straus (1980). It is found that this scheme also gives exactly the same results.

It is seen from Table 1 that there exist more than one steady state solution of the severely truncated system for the given forcing and dissipation. However, the question of stability of these steady states has not yet been answered. To answer this question partially, we carried out a stability analysis for these steady states with respect to first and second mode symmetric perturbations. At first we assumed that the perturbations are given by $\phi'_{1,3}(y,t) = \phi_{1,3}\,F_0(y)\exp(\sigma t)$ and $v'(y,t) = vF_1(y)\exp(\sigma t)$ and linearized the system of eqs. (4.5)–(5.7) around the steady states shown in Table 1. The growth rates are then found by solving the resulting eigenvalue problem. This procedure was

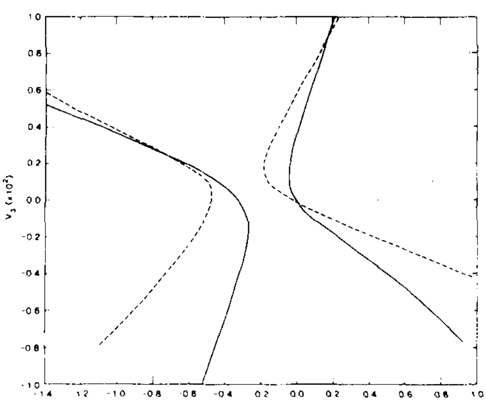

Fig. 3. The solid curve represents solution of eq. (5.3) while the dotted curve represents solution of eq. (5.6). The intersections represent solutions of the system of eqs. (5.1)–(5.6).

Table 1. *Common roots of eqs. (5.1)–(5.6). The zonal winds are obtained by using the geostrophic relations. τ_e is the e-folding time in days. All other quantities are in non-dimensional form*

Branch no.	V_1	V_3	$\phi_0^{(1)}$	$\phi_2^{(1)}$	$\phi_0^{(3)}$	$\phi_2^{(3)}$	$U_0^{(1)}$	$U_2^{(1)}$	$U_0^{(3)}$	$U_2^{(3)}$	Stability against symmetric perturbations: 1st γ-mode	Stability against symmetric perturbations: 2nd γ-mode
1	-0.169786×10^{-4}	-0.112019×10^{-3}	0.539748×10^{-3}	0.257112×10^{-1}	0.485818×10^{-4}	0.341555×10^{-4}	-0.374949×10^{-1}	0.514224×10^{-1}	-0.480246×10^{-4}	0.683111×10^{-4}	Stable $\tau_e \to \infty$	Stable $\tau_e \to \infty$
2	0.542920×10^{-1}	0.114250×10^{-2}	-3.241590	-0.602765	-3.612095	-0.239466	-3.073428	-1.205530	-5.869564	-0.678932	Stable $\tau_e \to \infty$	Unstable $\tau_e = 0.13$
3	-0.790000×10^{-2}	0.282250×10^{-2}	-0.672585×10^{-1}	0.173745	0.128864	0.236089	-1.117372	0.347492	0.391281	0.472199×10^{-1}	Unstable $\tau_e = 27.3$	Unstable $\tau_e = 22.3$
4	0.322481×10^{-1}	0.933141×10^{-2}	-1.897498	-0.262432	-1.962973	0.161190	-2.310456	-0.524864	-4.837777	0.322381	Stable $\tau_e \to \infty$	Unstable $\tau_e = 0.57$
5	-0.542400×10^{-1}	-0.141200×10^{-1}	-2.851552	-0.422538	-2.363566	-0.556899	-3.312871	-0.845075	-1.576836	-1.113798	Unstable $\tau_e = 4.7$	Unstable $\tau_e = 0.33$
6	0.199268×10^{-2}	0.956000×10^{-2}	-1.545864	2.767275	-0.491600	0.730345	-18.745990	5.534550	-5.114660	1.46069	Unstable $\tau_e = 69.9$	Unstable $\tau_e = 29.0$

repeated by assuming the perturbations to go as $\phi'_{1,3}(y,t) = \phi_{1,3} F_2(y)$ exp (σt) and $v'(y,t) = vF_3(y)$ exp (σt). The results of this analysis are also presented in Table 1. We find that, except for the first steady state, all the other steady states are unstable to either one or both types of perturbation. However, we note that the branches 3 and 6 can be considered quasi-stable with respect to these perturbations as the e-folding time of the perturbations for these states are more than three weeks. In order to have an idea of how stable these steady states are with respect to asymmetric perturbations, we calculated the quantity $q = \beta - U_{yy}$ for the branches 1, 3 and 6 over the whole domain of y and for both the levels. It is found that q does not change sign anywhere for the branch 1, while q changes sign somewhere within the domain for the branches 3 and 6. This suggests that branches 3 and 6 may be unstable to barotropic perturbations.

In order to have some insight into the nature of these steady states shown in Table 1, we grouped various terms in eqs. (5.1)–(5.6) in a physically meaningful way and calculated their magnitudes for all the steady states. For convenience, we have presented results of such calculations in Table 2 only for the first three steady states shown in Table 1. The momentum balances are actually exact. The residue that can be calculated from the numbers presented in Table 2 is merely a result of truncation. We note that the momentum balance for the branch 1 is mainly between the Coriolis term and friction which is essentially a linear balance. On the other hand, the non-linear momentum advection contributes significantly toward momentum balance for the branches 2 and 3 (as well as branches 4–6). Thus, branch 1 is locked near "linear resonance" while all the other branches represent various "non-linear resonances". The stability analysis of these steady states shows that only the steady state locked near linear resonance is stable against symmetric perturbations. Within the range of physical parameters used for this study, however, all the steady states representing non-linear resonances are unstable to symmetric perturbations.

As these results are for a very special system—a severely truncated system in which each variable is represented by only two orthogonal functions, we would like to know how reliable these results are. In other words, does a system in which each variable is represented by more than two orthogonal functions possess more than one equilibrium solution? To answer this question we shall numerically integrate the time dependent spectral equations with many more degrees freedom and using the severely truncated solutions as initial conditions. The results of these integrations are presented in the next section.

6. Numerical solutions

The time dependent spectral equations given by eqs. (4.5)–(4.7) are integrated using the following procedures. Given initial conditions for $\phi_j^{(1)}$ and $\phi_j^{(3)}$ for $j = 0, 2, \ldots, J$, the initial values of v_i for $i = 1, 3, \ldots, J + 1$ can be obtained by solving the $(J/2) + 1$ linear equations given by eq. (4.7). This is done by the standard matrix inversion method. Now, the right hand sides of eqs. (4.5) and (4.6) are known. Thus eqs. (4.5) and (4.6) represent $J + 2$ linear equations in $\dot{\phi}_j^{(1)}$ and $\dot{\phi}_j^{(3)}$ for $j = 0, 2, \ldots, J$. Using the standard matrix inversion method we solve this set of linear equations and obtain $\dot{\phi}_j^{(1)}$ and $\dot{\phi}_j^{(3)}$ for $j = 0, 2, \ldots, J$. Having obtained the time derivatives we use Matsuno's scheme to advance $\phi_j^{(1)}$ $\phi_j^{(3)}$ in time. Once new values of $\phi_j^{(1)}$ and $\phi_j^{(3)}$ are obtained, new v_i are calculated from eq. (4.7) and the sequence is repeated. The interaction coefficients defined by eq. (4.8) must be calculated only once. They are calculated in the beginning of the program and stored. The physical parameters used in the numerical integrations are the same as those used for the analytic calculation of the steady state solutions (Section 5).

All numerical calculations are performed for thermal forcing corresponding to $T_e(y) = [\alpha_0 T_0 + \alpha_2 T_2 H_2] \exp(-y^2/2)$ where $T_0 = 40$, and $T_2 = 20$. This equilibrium temperature distribution is shown in Fig. 1. This thermal forcing represents an earth with maximum surface temperature at about 25° N and 25° S on both sides of the equator. Within the framework of our truncated representation, this thermal forcing is expected to represent conditions close to monsoon conditions.

6.1. *Linear solutions: two-layer spectral model*

As a test of our numerical model, we first dropped the non-linear terms in eqs. (4.5)–(4.7) and integrated them numerically until the solution converged to a steady state. Comparison of the linear steady states thus obtained with an analytic-

Table 2. *Momentum and heat balances for the first three branches shown in Table 1*

Branch no.	Equation for mode (k)	Momentum balance (Level-3): Relative momentum advection	Momentum balance (Level-3): Coriolis term	Momentum balance (Level-3): Friction	Momentum balance (Level-3): Residual	Momentum balance (Level-1): Relative momentum advection	Momentum balance (Level-1): Coriolis term	Momentum balance (Level-1): Friction	Momentum balance (Level-1): Residual	Heat balance: Adiabatic compression expansion	Heat balance: Thermal heating	Heat balance: Residual
1	0	-0.306972×10^{-6}	-0.287549×10^{4}	0.290619×10^{-4}	0.0	-0.305024×10^{-6}	-0.287549×10^{4}	0.290600×10^{-4}	0.0	-0.345242×10^{5}	0.345261×10^{5}	0.192249×10^{-9}
	2	-0.111909×10^{-5}	-0.167083×10^{3}	0.168202×10^{3}	0.0	-0.399061×10^{-6}	-0.167083×10^{-3}	0.167482×10^{-3}	0.0	0.149885×10^{4}	-0.149787×10^{-4}	0.982313×10^{-8}
2	0	-0.161028×10^{1}	0.146437×10^{1}	0.145908×10^{-2}	0.0	-0.390168×10^{1}	0.146437×10^{-1}	0.243731×10^{2}	0.0	-0.247324×10^{2}	0.247348×10^{2}	0.233685×10^{-6}
	2	-0.425583×10^{-1}	0.422932×10^{1}	0.265115×10^{3}	0.0	-0.799927×10^{-1}	0.422932×10^{-1}	0.376995×10^{-1}	0.0	-0.152870×10^{3}	0.152417×10^{-3}	-0.453155×10^{-6}
3	0	0.175627×10^{2}	-0.150758×10^{2}	-0.248690×10^{3}	0.0	0.620501×10^{3}	-0.150758×10^{-2}	0.887078×10^{-3}		0.477162×10^{3}	-0.476300×10^{3}	0.861715×10^{-6}
	2	0.171195×10^{-2}	-0.210343×10^{2}	0.341481×10^{-3}	0.0	0.601511×10^{3}	-0.210343×10^{2}	0.150192×10^{-2}	0.0	-0.377660×10^{3}	0.370685×10^{-3}	-0.697502×10^{-5}

ally calculated linear steady state (Section 3) is expected to give an idea of the working of our numerical model. An interesting point to note here is that, for a given thermal forcing and for a given set of physical parameters, the model goes to the same steady state no matter what initial condition we choose. This result is consistent with the fact that in the absence of the non-linear terms, there is nothing that can produce degeneracy in the model.

The linear steady state obtained from the numerical model (in which 10 orthogonal functions were used to represent each variable) for thermal forcing corresponding to $T_e(y) = [\alpha_0 T_0 + \alpha_0 T_2 H_2] \exp(-y^2/2)$ where $T_0 = 40$ and $T_2 = 20$, was compared with the analytically obtained steady state for the same thermal forcing presented in Fig. 2. It is seen that the agreement between the numerical and analytical results is excellent. Within the resolution of the Figs. 2a and 2b, the meridional winds as well as the zonal winds at the upper layer obtained from the numerical model fit in exactly with those obtained from the analytical solution. As expected, the numerical model also gives $u_3 = 0$ ($|u_3|_{max} < 1$ cm s^{-1}). The upper level zonal wind in the linear model and for this thermal driving is easterly near the equator and westerly in the middle latitude. The meridional circulation for this state has two cells with a descending branch around the equator, an ascending branch around 30 degrees latitude and another descending branch around 70 degrees latitude.

6.2. *Non-linear solutions: two-layer spectral model*

In this section, we present results of numerical integrations of the full non-linear equations given by eqs. (4.5)–(4.7). At first, we took five orthogonal functions to represent each variable (viz., j, $k = 0, 2, 4, 6, 8$ and $i = 1, 3, 5, 7, 9$) and integrated eqs. (4.5)–(4.7) with various initial conditions given by the truncated steady states shown in Table 1. The physical parameters used in these numerical calculations are the same as those used for the severely truncated analytic solutions (Section 5). It is found that the model converges to only one steady state no matter what initial condition we choose from Table 1. In order to see the effect of truncation, we then doubled the number of orthogonal functions to represent each variable (viz., s, $k = 0, 2, \ldots, 18$ and $i = 1, 3, \ldots, 19$) and integrated the model again with initial conditions given by the truncated steady state shown in Table 1. Again we find that the model converges to only one steady state. This steady state is similar to the steady state obtained from the five function model. But the two steady states are not identical, showing that five functions are not sufficient to represent the system. It is found that the addition of a few more functions to the ten function model, however, does not change the final steady state significantly. Thus, the steady state to be discussed below in detail is the one obtained from the ten function model.

The meridional velocity at the lower layer, the zonal winds at the upper layer, the zonal winds at the lower layer and the equilibrium temperature distribution for the steady state obtained from the numerical model are shown in Fig. 4. The meridional circulation for this steady state has descending motion between the equator and 15° N, ascending motion between 15° N and 40° N and descending motion thereafter. The magnitude of the meridional winds associated with this steady state is small (in cms). This is attributed to the absence of zonal mean pressure gradient in the model. As a result, the meridional velocity is not determined by geostrophic balance. In this case, the Coriolis term is balanced by the residual of the rest of the terms (also see Hunt, 1973). We note that the meridional winds for the non-linear steady state is remarkably similar to the meridional winds for the linear steady state (Fig. 2a). The zonal winds at the upper level are also very similar to the zonal winds at the upper level for the linear state (Fig. 2b). However, unlike the linear steady state for which the zonal winds at the lower level were extremely small, the zonal winds at the lower level for the non-linear steady state are appreciable. We also note that unlike the linear steady state for which $u_1 = u_3 = 0$ at the equator, $u_1 \neq u_3 \neq 0$ for the non-linear state at the equator. This is in agreement with the momentum balance requirement near the equator. For a descending motion over the equator ($\omega_2 > 0$), eqs. (2.1), (2.2), (2.9) and (2.10) demand that $u_1 = (A + 2k_i)\, u_3/2k_i$. This is satisfied by the non-linear steady state obtained by numerical integration. The zonal winds and the temperature distribution for this steady state also satisfy a thermal wind relation.

The steady state obtained from the numerical integration of the multimode time dependent equations is quite similar to the stable steady state obtained from the severely truncated system

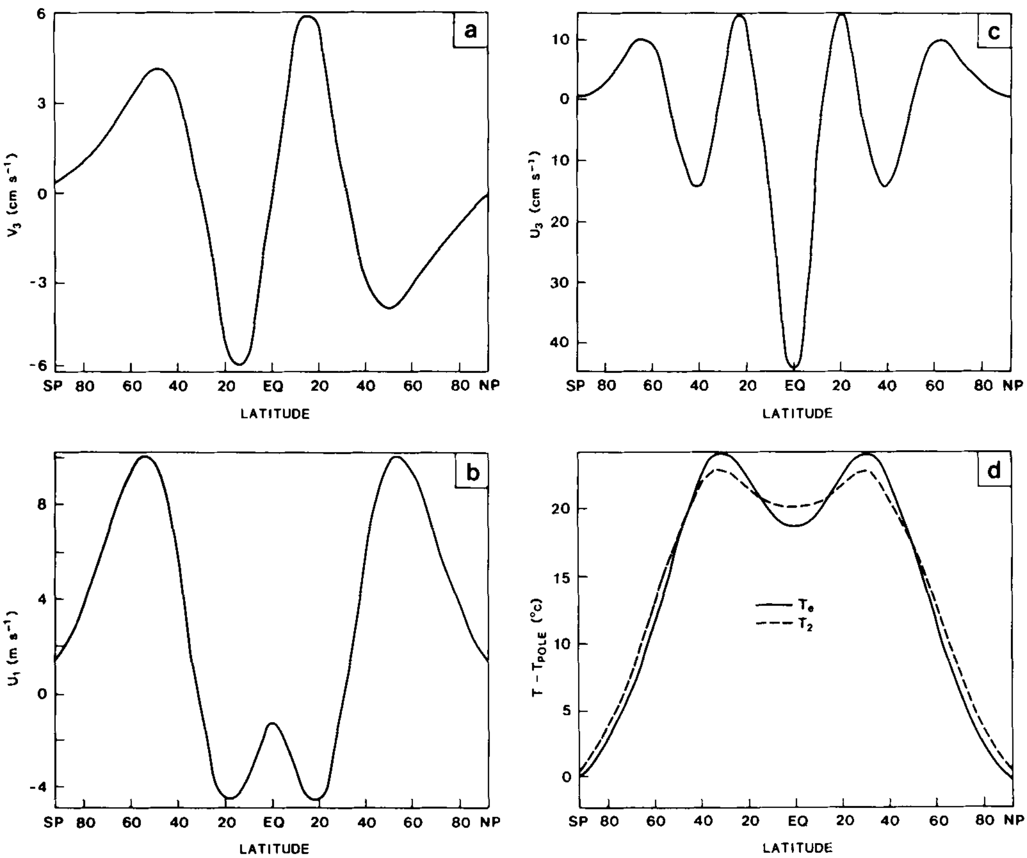

Fig. 4. Steady state solution for the non-linear spectral model (a) Meridional wind. (b) Zonal wind at the upper layer. (c) Zonal wind at the lower layer. (d) Temperature distribution for the steady state as compared to the radiative equilibrium temperature. The physical parameters for this steady state are the same as in the linear solution.

(branch 1 in Table 1). This means that this steady state is not only stable against first and second y-mode perturbations, it is stable against higher y-mode perturbations as well. The inability of the multimode numerical model to show any other steady state seems to be due to the fact that all the other steady states shown by the truncated system are unstable to symmetric perturbations.

6.3. *Non-linear solutions: multi-layer grid point model*

In this section, we examine the possibility of existence of multiple equilibria in a simple multilayer axi-symmetric model. In this regard, we had the opportunity to examine a model developed by Kalnay-Rivas (1973). This is a grid point model with primitive equations on a sphere under Boussinesq approximation.

We adapted this model for representing the earth's atmosphere by introducing appropriate forcings and physical parameters. A thermal forcing in the form of a Newtonian cooling law is introduced. The prescribed radiative equilibrium temperature is shown in Fig. 5a. This radiative equilibrium temperature distribution is chosen in such a way that it is similar in structure with the one prescribed for our two-layer model (Fig. 1). Under the Boussinesq approximation, the radiative temperature distribution can be replaced by a radiative equilibrium density distribution. We also intro-

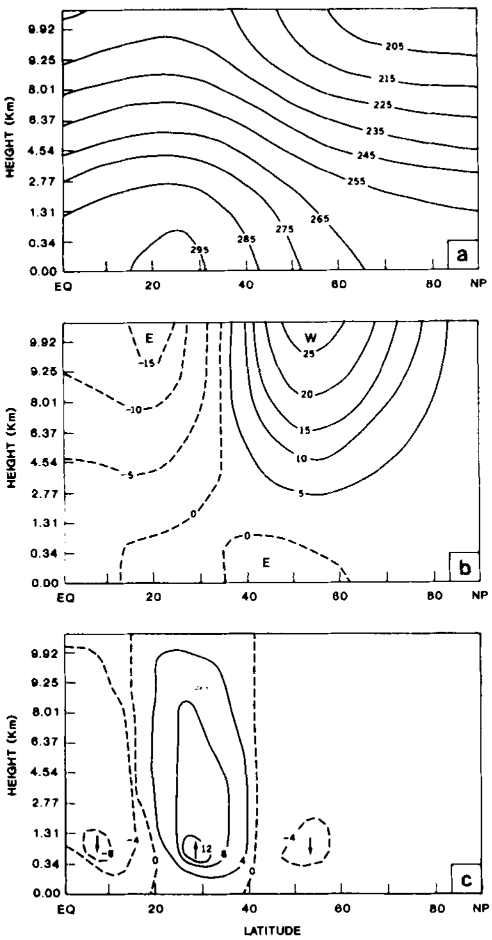

Fig. 5. Steady state from the multi-level grid point model. (a) Prescribed radiative equilibrium temperature distribution. The contour intervals are 10 K. (b) Zonal wind distribution. The contour intervals are 5 m s^{-1}. (c) Vertical velocity distribution. The contour intervals are 4×10^{-2} cm s^{-1}.

duced a surface drag low as a bottom boundary condition. The boundary conditions used are

$$W = 0, \quad \frac{\partial u}{\partial Z} = 0, \quad \frac{\partial v}{\partial Z} = 0, \quad \frac{\partial p}{\partial Z} = 0: \qquad \text{at } Z = H$$

$$W = 0, \quad \nu_V \frac{\partial u}{\partial Z} = Cu; \quad \nu_V \frac{\partial v}{\partial Z} = Cv, \quad \frac{\partial p}{\partial Z} = 0: \qquad \text{at } Z = 0$$

$$v = 0, \quad \frac{\partial u}{\partial y} = 0: \qquad \text{at the equator}$$

$$u = 0, \quad v = 0. \qquad \text{at the poles}$$

The physical parameters used in the model are. a = radius of the earth = 6.37×10^6 m: H = equivalent depth of the atmosphere = 10 km. g = acceleration due to gravity = 9.81 m s^{-2}: $C = 0.02$ m s^{-1}, $\nu_H = K_H = 5 \times 10^4$ m^2 s^{-1}: $\nu_V = K_V = 1.5$ m^2 s^{-1} where K_H and K_V are horizontal and vertical coefficients of eddy diffusivity and ν_H and ν_V are corresponding coefficients of eddy viscosity. A small amount of horizontal diffusion is necessary in the model for stability. However, it is seen that $\nu_V/H^2 > 12\nu_H/a^2$, showing that the strength of the horizontal diffusion is much weaker compared to the vertical diffusion. The present version of the model does not have cumulus heating and it has 18 grid points from equator to the pole and 17 levels in the vertical.

With the above-mentioned physical parameters and thermal forcing, the model was integrated for a large number of initial conditions. However, we always obtained the one and the same steady state. The zonal winds and the vertical velocity for this steady state are presented in Figs. 5b and 5c. The meridional circulation for this state has two cell structure with a descending branch near the equator, an ascending branch around 30° N and another descending branch around 50° N. This is a thermally direct circulation. Surface zonal winds are weak easterlies in tropics (from the equator to 15° N), weak westerlies in subtropics (from 15° N to 35° N), easterlies between 35° N and 62° N and again westerlies in the polar region. Upper level zonal winds are easterly in the tropics and subtropics and westerly in the middle and high latitudes. It is interesting to note that both the zonal winds and meridional circulation for this steady state have a striking similarity to the zonal winds and meridional circulation for the steady state obtained with the two-layer spectral model.

7. Conclusions and remarks

Using simple models, we have examined the possible existence of multiple equilibria in axisymmetric circulations. An analytic solution of the severely truncated version of the two layer spectral model shows that there exist several steady states. However, an analysis of stability of these steady states with respect to first and second y-mode perturbations shows that one of these steady states is stable against both type of perturbations, while two other steady states are found to be quasi-stable with respect to these perturbations. The time dependent equations for the two-layer spectral model with many more degrees of freedom was then integrated with various initial conditions. This shows that the model converges to only one steady state similar to the stable steady state obtained with the severely truncated system. Several integrations were also performed with a multi-level grid point model. This model also is found to give only one steady state. For forcing and dissipation similar to ones used in the two-layer spectral model, the steady state obtained with the multilevel grid point model is very similar to the steady state obtained with the two-layer model.

Thus, the simple models used in this study failed to show the existence of multiple equilibria in symmetric circulations. A question can be raised at this point. Is there a range of thermal forcing or dissipation parameters for which there exist multiple equilibria in these models? This question was examined in the context of the severely truncated version of our model. We calculated the non-linear steady states of the truncated system for a wide range of thermal forcings and a wide range of other physical parameters (e.g., D, A, k_i, and k_r). From this study, we find that, qualitatively, the result remains the same. In other words, we always find only one stable solution.

In our spectral model, the effect of surface friction on the lower layer, is parameterized in terms of surface wind extrapolated from the lower layer, i.e., u_3 (eq. (2.16)). In such two-layer models, the surface wind is often extrapolated from the winds at both the layers instead of just the wind at the lower layer. A linear extrapolation for this problem may be written as (Yao, 1980)

$$u_s = \tfrac{3}{2}u_3 - \tfrac{1}{2}u_1$$

With this modified form of surface friction parameterization, we re-examined our results with the truncated version of our spectral model. We calculated all the non-linear steady states. However, it is again found that, only one of the steady states is stable against symmetric perturbations.

Although the models used in the study failed to show the existence of multiple equilibria in symmetric circulations, we must remember that some important physical processes are not represented by these models. For example, it is well known that the cumulus convection plays an important role in maintaining the tropical circulation. The parameterization for cumulus convection used in this study is at best heuristic. The effect of heating due to cumulus convection appears in our model only through the static stability parameter. Moreover, we know that the transport of heat and momentum by eddies contributes significantly in maintaining the mean meridional circulation. These eddy processes are also absent in our model. Also, our model does not have any mountains nor does it have any land-ocean contrast. We believe that the absence of these physical processes is responsible for the inability of these models to exhibit multiple equilibria in symmetric circulations.

The parameterizations of the physical processes in our simple models are not adequate to represent the details of the tropical atmosphere properly. Therefore, our conjecture that the active and break phases of South Asian monsoon may be two equilibrium states of the tropical atmosphere, remains to be verified. This question must be examined using more realistic models with more realistic parameterizations of the physical processes.

8. Acknowledgements

This problem was suggested to me by Professor Jule Charney and I am extremely grateful to him for his encouragement and for a large number of stimulating discussions. I would like to thank Drs. D. Andrews, E. Kalnay, E. Sarachik, and E. Schneider for discussions at various stages of the work. Special thanks are due to Dr. J. Shukla for his constant encouragement throughout the course of this work. Part of this work was carried out when the author was a Post-doctoral Research Associate at the Department of Meteorology and Oceanography at M.I.T., under National Science Foundation Grant ATM. 76-20070.

REFERENCES

Abramowitz, M. and Stegun, I. A. 1965. *Handbook of mathematical functions*, New York, Dover, 1046 pp.

Bates, J. R. 1970. Dynamics of disturbances on the Intertropical Convergence Zone. *Quart. J. Roy. Met. Soc. 96*, 677–701.

Cane, M. A. and Sarachik, E. S. 1976. Forced baroclinic ocean motions. I. The linear equatorial unbounded case. *J. Mar. Res. 34*, 629–665.

Charney, J. G. 1969. The intertropical convergence zone and the Hadley circulation of the atmosphere. Proc. of WMO/IUGG Symposium of NWP in Tokyo, Met. Soc. Japan, pp. III-73–79.

Charney, J. G. and DeVore, J. G. 1979. Multiple flow equilibria in the atmosphere and blocking. *J. Atmos. Sci. 36*, 1205–1216.

Charney, J. G. and Straus, D. M. 1980. Form-drag instability, multiple equilibria and propagating planetary waves in baroclinic orographically forced planetary wave systems. *J. Atmos. Sci. 37*, 1157–1176.

Gilchrist, A. 1977. The simulation of the Asian summer monsoon by general circulation models. *Pageoph 115*, 1431–1448.

Hahn, D. G. and Manabe, S. 1975. The role of mountains in the South Asian monsoon circulation. *J. Atmos. Sci. 32*, 1515–1591.

Hamilton, M. G. 1977. Some aspects of break and active monsoon over Southern Asia during summer. *Tellus 29*, 335–344.

Held, I. M. and Hou, A. Y. 1980. Nonlinear axially symmetric circulations in a nearly inviscid atmosphere. *J. Atmos. Sci. 37*, 515–533.

Hunt, B. C. 1973. Zonally symmetric global general circulation models with and without hydrologic cycle. *Tellus 25*, 337–354.

Kalnay-Rivas, E. 1973. Numerical model of the circulation of the atmosphere of Venus. *J. Atmos. Sci. 31*, 763–779.

Keshavamurty, R. N. 1973. Power spectra of large scale disturbances of the Indian South West monsoon. *Indian J. Met. Geophys. 24*, 117–124.

Krishnamurti, T. N. and Bhalme, H. N. 1976. Oscillations of a monsoon system. Part I: observational aspects. *J. Atmos. Sci. 33*, 1937–1954.

Krishnamurti, T. N., Kanamitsu, M., Ceselski, B. and Mathur, M. B. 1973. Florida State University's Tropical Prediction Model. *Tellus 25*, 523–535.

Murakami, M. 1976. Analysis of summer monsoon fluctuations over India. *J. Met. Soc. of Japan 54*, 15–31.

Oort, A. H. and Rasmusson, E. M. 1971. Atmospheric Circulation Statistics, U.S. Department of Commerce, NOAA Professional Paper No. 5, NTIS No. AD739.434.

Ramamurthy, K. 1969. Some aspects of the break in the southwest monsoon during July and August. *Forecasting Manual, Part IV* (18.3). India Meteorological Department, New Delhi, India.

Schneider, E. K. and Lindzen, R. S. 1977. Axially symmetric steady state models of the basic state for instability and climate studies. Part I: Linearized calculations. *J. Atmos. Sci. 34*, 263–279.

Schneider, E. K. 1977. Axially symmetric steady state models of the basic state for instability and climate studies. Part II: Nonlinear calculations. *J. Atmos. Sci. 34*, 280–296.

Sikka, D. R. and Gadgil, S. 1980. On the maximum cloud zone and the ITCZ over Indian longitudes during Southwest monsoons. *Mon. Wea. Rev. 108*, 1840–1853.

Washington, W. M. and Daggupati, S. M. 1975. Numerical simulation with NCAR global circulation model of the mean conditions during Asian-African summer monsoon. *Mon. Wea. Rev. 103*, 105–114.

Webster, P. J., Chou, L. and Lau, K. M. 1977. Mechanisms effecting the state, evolution and transition of the planetary scale monsoon. *Pageoph 115*, 1463–1491.

Webster, P. J. and Chou, L. 1980a. Seasonal structure of a simple monsoon system. *J. Atmos. Sci. 37*, 354–367.

Webster, P. J. and Chou, L. 1980b. Low frequency transitions of a simple monsoon system. *J. Atmos. Sci. 37*, 368–382.

Yao, M. S. 1980. Maintenance of quasi-stationary waves in a two-level quasi-geostrophic spectral model with topography. *J. Atmos. Sci. 37*, 29–43.

Yashunari, T. 1979. Cloudiness fluctuations associated with northern hemisphere summer monsoon. *J. Met. Soc. Japan 57*, 227–242.